ACS APPLIED MATERIALS & INTERFACES

RESEARCH ARTICLE

www.acsami.org

Ohmic Contact of Cadmium Oxide, a Transparent Conducting Oxide, to n-type Indium Phosphide

Fang Ou,[†,*] D. Bruce Buchholz,[‡] Fei Yi,[†] Boyang Liu,[†] Chunhan Hseih,[†] Robert P. H. Chang,[‡] and Seng-Tiong Ho[†]

[†]Department of Electrical Engineering and Computer Science, Northwestern University, Evanston, Illinois 60208, United States

[‡]Department of Material Science and Engineering, Northwestern University, Evanston, Illinois 60208, United States

Supporting Information

ABSTRACT: Good ohmic contact to n-type indium phosphide (n-InP) with cadmium oxide (CdO), a transparent conducting oxide (TCO), has been achieved. Hydrogen plasma surface pretreatment of the n-InP substrate, prior to the pulsed laser deposition (PLD) of the CdO film, is key to achieving ohmic contact. On substrates pretreated with a hydrogen plasma, contact resistances as low as $(6.8 \pm 2.8) \times 10^{-6}$ Ω cm^2 are obtained.

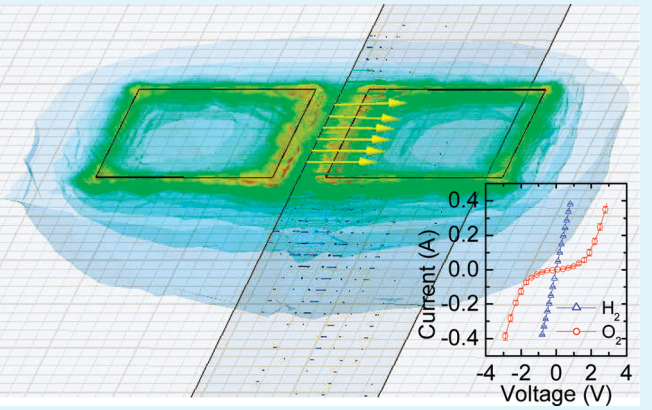

KEYWORDS: Ohmic contact, CdO, TCO, PLD, III−V semiconductor, surface pretreatment

INTRODUCTION

Devices fabricated from InP, such as field effect transistors,[1−3] heterojunction bipolar transistors,[4−6] and high electron mobility transistors,[7−9] require high-conductivity ohmic contacts. Additionally, photonic InP devices, such as solar cells[10−12] and light emmitting diodes,[13−15] would benefit from contacts that were optically transparent. Although the large band gaps usually associated with optical transparency preclude the possibility of high conductivity in many transparent materials, a number of metal oxides, known as transparent conducting oxides (TCOs), possess the unique properties of being both transparent and highly conductive. In this paper, we look at the formation of an optically transparent, highly conductive, ohmic-contact to n-type InP (n-InP).

Metal cations with filled d-shells comprise the highest performance and most commercialized n-type TCOs. The filled d-shell precludes the possibility of d→d interband transitions, which can be optically absorbing. Most prominent of the cations used in TCOs are Zn^{2+}, Cd^{2+}, In^{3+}, Sn^{4+}, and to a lesser extent Ga^{3+} because of the relatively large band gap and poor conductivity of its oxides.[16−18] For many applications in the visible spectrum, the optical band gap of cadmium oxide (CdO)-based TCOs is considered marginally adequate, ranging from 2.2 to 3.3 eV.[19−21] However, for long wavelength-based InP devices, the band gap is more than adequate.[22−24] Compared to the majority of TCOs, CdO does not need extrinsic doping, as its natural donor defects, which are most likely oxygen vacancies,[25] and its high carrier-mobility lead to very good conductivity,[19] and epitaxially grown CdO-based TCOs have exhibited conductivities of 42000 S/cm with mobilities greater than 600 cm^2/V s.[26]

High speed and wide bandwidth devices, many of which employ InP-based materials, require contact materials that minimize the dc voltage drop and RC time constant.[27,28] As many of these high-speed devices are for optoelectronic applications that would benefit from a TCO contact material,[22] the high conductivity of CdO-based TCOs make them an ideal candidate material. The low refractive index of CdO ($n \approx 2$) relative to InP ($n \approx 3.2$) also possesses the possibility that CdO could be used as a conducting waveguide cladding material for current injection into high refractive index contrast nanophotonic devices.[23,29] A critical concern for these applications, however, is the electrical properties across the interface between the contact material and semiconductor. It is of primary importance that the resistance across this interface be minimized and the contact be ohmic.[27,30] No matter how transparent and conductive a material might be, if a proper interface cannot be constructed, the material is useless as a contact material. In this paper, we focus on the electrical properties across the interface between the contact material, CdO, and the semiconductor, n-InP.

A primary consideration in the formation of an ohmic contact is the relative position of the metal (or TCO) and semiconductor Fermi levels. For ohmic contact to an n-type nondegenerate semiconductor, it is generally required that the Fermi level of the

Received: January 31, 2011
Accepted: March 28, 2011
Published: March 28, 2011

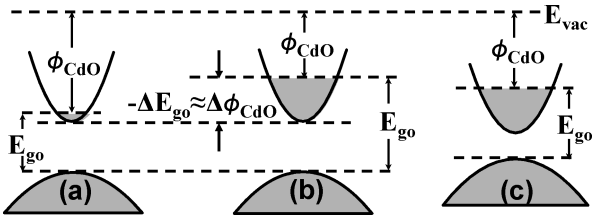

Figure 1. Schematic diagram of the energy levels in donor-doped CdO: (a) Nominally undoped CdO; (b) n-type doped CdO showing only the effect of conduction-band filling; (c) n-type doped CdO showing the effect of both conduction band filling and many body interactions.

metal (ϕ_{CdO}) be less than that of the semiconductor (ϕ_{InP}).[31,32] For both CdO and InP, the Fermi levels depend on the degree of doping. For the donor-doped n-InP, ϕ_{InP} will be close to the conduction band minimum (CBM) of 4.4 eV.[33] The unperturbed CBM for CdO is ~4.6 eV,[34] and CdO needs to be doped such that ϕ_{CdO} is moved ~0.2 eV closer to the vacuum level for an ohmic contact to be formed. This, however, appears to be easily done.

The increase in the optical band gap (E_{go}) by doping can be used as a conservative first approximation for the decrease in ϕ_{CdO}. Donor-doping of CdO results in two competing effects on both E_{go} and ϕ_{CdO}. The first is the filling of the conduction band that lowers ϕ_{CdO} ($\Delta\phi_{CdO}$);[35,36] this also results in the well-known Burstein−Moss widening of the optical band gap (ΔE_{go})[37,38] and $-\Delta E_{go} \approx \Delta\phi_{CdO}$. The second is the many body interactions that shift both the valence band maximum (VBM) closer to the vacuum level (E_{vac}) and the CBM further from E_{vac}.[39] Hence, $-\Delta E_{go} < \Delta\phi_{CdO}$, see Figure 1. The unperturbed direct band gap of CdO has been calculated as 2.2 eV,[40] which agrees well with the measured E_{go} of lightly (~10^{19} cm^{-3}) doped CdO.[41,42] Using ΔE_{go} as a first approximation for $\Delta\phi_{CdO}$, an E_{go} > 2.4 eV would be indicative of a ϕ_{CdO} < 4.4 eV. Values of E_{go} > 2.4 eV have been reported for intrinsically doped CdO[20,43,44] and E_{go} > 2.8 eV for donor-doped CdO.[26]

EXPERIMENTAL SECTION

In the experiment, contacts to n-InP from both intrinsically doped and Sn-doped CdO (henceforth call CdO and CdO:Sn, respectively) are examined. Thin-film CdO and CdO:Sn were grown by pulsed laser deposition (PLD). A 248 nm KrF excimer laser with a 25 ns duration operated at 2 Hz and a beam energy set to 200 mJ/pulse was used. The beam was focused to a 1 mm ×2 mm spot on the target material. CdO was deposited from a CdO target and the tin dopant from a SnO_2 target. A computer-controlled shuttle was used to alternate ablation between the CdO and SnO_2 targets. Less than one monolayer was deposited in a typical CdO−SnO_2 cycle to help ensure a uniform distribution of Sn in the film. The target substrate separation was 8 cm. During deposition, the substrates were heated to 200 ± 5 °C by a resistively heated holder. The substrates were attached to the substrate holder with silver paint; previous characterization of the substrate holder in this temperature range showed that the surface temperature of the substrate was within 3 °C of the substrate holder temperature. The deposition ambient was 2 mTorr UHP oxygen. Films were grown on both 650 μm thick ĉ-sapphire and 350 μm thick n-type (S-doped) InP (100).

Prior to film deposition, all substrates were solvent cleaned: 3 min acetone, 3 min isopropylalcohol, and 3 min deionized water ultrasonic bath. Substrates that received only this clean are referred to as "solvent cleaned". Subsequent to the solvent clean some substrates were cleaned by reactive ion etching in an Oxford Instrument Plasma Lab μP80

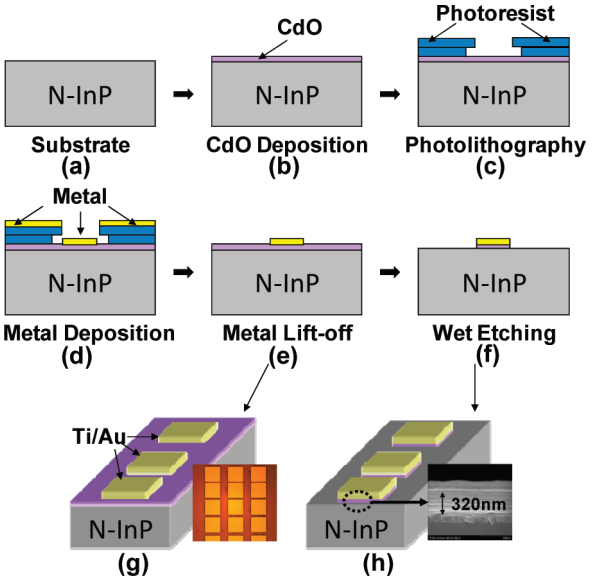

Figure 2. Schematic representation of the fabrication process used to define the CdO/n-InP contact measurement pattern.

(1 min, 100 W, 75 mTorr) in an oxygen atmosphere (50 sccm O_2) and other substrates in a hydrogen atmosphere (50 sccm H_2); these are referred to as "O_2 plasma cleaned" and "H_2 plasma cleaned", respectively.

The films deposited on ĉ-sapphire were used for film assay, Hall measurements, and optical absorption measurements. The metal assay was measured by energy-dispersive X-ray analysis (EDAX) using a FEI Ouanta 600F scanning electron microscope (SEM) fitted with an Oxford Instruments X-Sight Model 6427 EDAX system. The sheet resistance (Ω/□), areal carrier concentration (1/cm^2), and carrier mobility (cm^2/V s) were measured with a Bio-Rad HL5500PC Hall system on samples in the van der Pauw geometry. The carrier concentration (1/cm^3) and resistivity (Ω cm) were calculated by dividing the areal carrier concentration and multiplying the sheet resistance by the film thickness. Optical transparency and reflectivity were measured between 250 and 2400 nm with a Perkin-Elmer Lambda 1050 fitted with a 150 mm integrating sphere that was used for both transmission and reflection measurements in the dual-beam mode. Absorbance (A) was derived from the transmission spectra corrected for reflection as described in the Supporting Information of ref 44. The optical absorption coefficient (α: 1/cm) was calculated by dividing the absorbance by the film thickness. The film thickness was determined by cross sectional SEM.

To determine the interfacial properties between the CdO (CdO:Sn) film and n-InP substrate, contact patterns were defined on the n-InP samples as illustrated in Figure 2. After CdO (CdO:Sn) deposition (Figure 2b), photolithography was used to define a linear array of 200 μm × 200 μm pads with increasing gap distance (10−60 μm gap in 10 μm increments) between adjacent pads (Figure 2c). Ti (10 nm) followed by Au (300 nm) was deposited by e-beam evaporation (Figure 2d), followed by a lift-off process to define the metal pads (Figure 2e). A $NH_3 \cdot H_2O$ wet etch, using the contact metal as an etch stop, was used to remove the exposed CdO (CdO:Sn) and complete the contact structure (Figure 2f). A schematic depiction and a top-view micrograph of the metal contact pattern on the CdO (CdO:Sn) thin film are shown in panel (g) of Figure 2. The electrical properties of the CdO (CdO:Sn) contacts to the n-InP were measured with a digital source meter (Keithley 2400). The sample was placed on an insulating stage, and two adjacent pads were connected to the source meter via two microprobes. A voltage was applied, and the resultant current measured ($I-V$ curve).

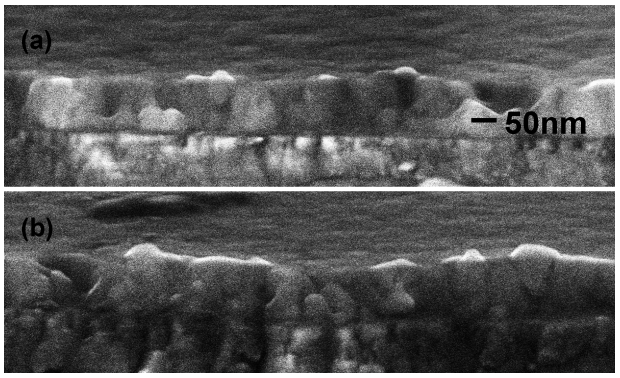

Figure 3. SEM images of a 100 nm thick CdO film deposited on ĉ-sapphire by PLD: (a) CdO; (b) CdO:Sn.

Table 1. Electrical and Optical Properties of the CdO and CdO:Sn Films

Sn conc. (atomic %)	0%	1%
conductivity (S/cm)	2000 (±200)	7600 (±800)
Hall mobility (cm^2/V s)	85 (±6)	107 (±7)
carrier conc. (cm^{-3})	$(1.5 \pm 0.4) \times 10^{20}$	$(5.6 \pm 1.6) \times 10^{20}$
optical loss −1550 nm (cm^{-1})	5000 (±500)	9000 (±900)
optical band gap (eV)	2.4	2.5

RESULT AND DISCUSSION

The films, as deposited on n-InP, are of uniform thickness (∼100 ± 5 nm), dense, and have a large grain size (∼50 nm), see Figure 3. Both CdO and CdO:Sn films show good conductivity for a TCO, particularly for one deposited at such a low temperature, see Table 1. The carrier concentrations are what might be expected for CdO and CdO:Sn.[26,46,47] The carrier mobility is lower than in the highest-quality single-crystal-like films (which can exceed 600 cm^2/V s)[26] and can reasonably be attributed to an increased density in grain boundaries.[48,49] The mobilities, on the order of 100 cm^2/ V s, are still quite high for a TCO, particularly for one deposited at such a low temperature. The electron mobility of the CdO:Sn film exceeds that of the CdO film, even though the films have comparable grain sizes, see panels (a) and (b) of Figure 3, and it has been proposed that the Sn-doping can lower the potential barrier height at the grain boundaries.[25,50,51]

The transmittance and reflectance spectra of the CdO and CdO:Sn samples are shown in panel (a) of Figure 4. A shift of the band edge to higher energy (smaller wavelength) is clearly visible for CdO:Sn relative to CdO, consistent with the higher carrier concentration in the CdO:Sn film and the expected Burstein−Moss widening of the optical band gap. The majority of transmittance loss between 1000 nm and the band edge for both samples is due to reflectance; this is most easily seen by comparing the transmittance spectra in panel (a) of Figure 4 to the absorbance data presented in panel (b) of Figure 4. Above ∼1000 nm, the effects of free carrier absorption can be observed with the higher absorption for CdO:Sn than CdO films. The optical band gap of the films, Table 1, is determined from optical absorption spectra. CdO is a direct band gap material; therefore the optical band gap can be determined from a plot $(\alpha h\nu)^2$ verses $h\nu$ plot extrapolated to the ordinate intercept (where α is the optical absorption coefficient at energy $h\nu$). The values for the band gap are consistent with those found in the literature for

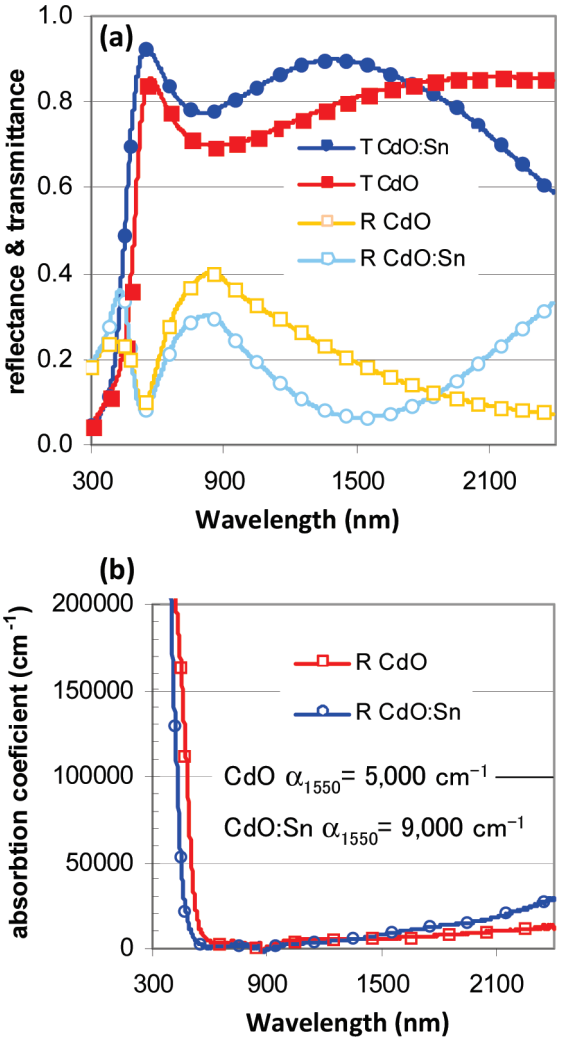

Figure 4. (a) Transmittance and reflectance spectrum for CdO and CdO:Sn. (b) Absorption coefficient as a function of wavelength for CdO and CdO:Sn.

equivalent carrier concentrations.[20,26,52] The band gaps also indicate that the Fermi levels of the CdO films should be shifted sufficiently to allow ohmic contact to the InP substrates.

For the substrates that were only solvent cleaned, the contact formed between the n-InP and both the CdO and CdO:Sn exhibit Schottky behavior as shown in panel (a) of Figure 5. The pretreatment/cleaning of a semiconductor prior to contact material deposition can have a strong effect on the contact's electronic properties.[53,54] To preclude the possibilities of trace organics being left at the interface prior to CdO deposition, the InP was O_2 plasma cleaned. The resulting contacts still exhibited Schottky behavior and were more resistive than those formed by solvent cleaning as shown in panel (b) of Figure 5. It can also be observed that the CdO:Sn contacts exhibit a higher resistance than the CdO contacts.

The Schottky behavior indicates the possibility of the existence of an interfacial oxide layer. To analyze the effect, a reasonable treatment is to consider the surface layer to be In_2O_3.[55] The free-band diagram of CdO, In_2O_3, and n-InP is drawn schematically in panal (a) of Figure 6.[35] Before CdO deposition, electrons flow from the n-InP into the interfacial oxide layer bending

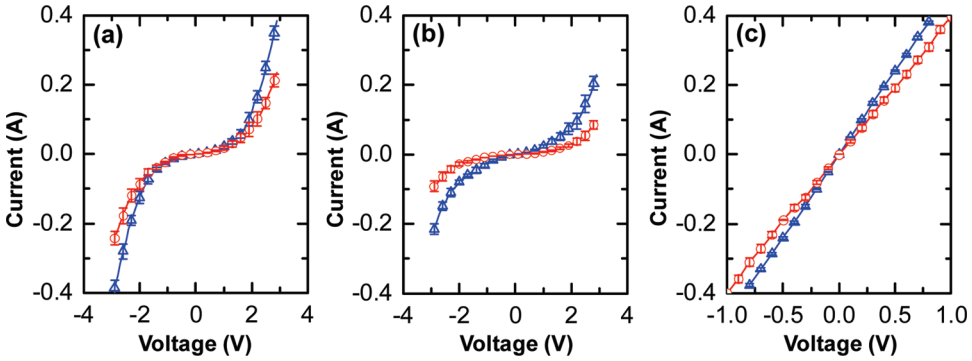

Figure 5. Current−voltage measurements for CdO (blue triangles) and CdO:Sn (red circles) contact structures on n-InP; (a) solvent cleaned; (b) O_2 plasma cleaned; (b) H_2 plasma cleaned.

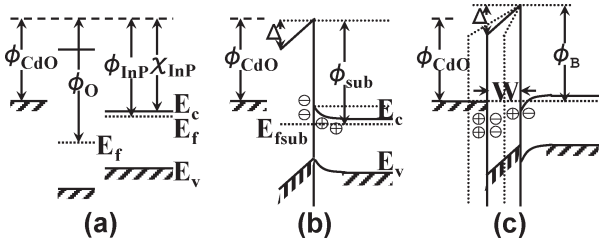

Figure 6. Band diagram for (a) isolated CdO, the oxide layer and the n-InP; (b) n-InP with oxide on the surface; (c) CdO contact to the n-InP with the interfacial oxide layer.

the band structure as shown in panel (b) of Figure 6. The equivalent work function for the n-InP substrate is now ϕ_{sub}. When CdO is brought into contact with the interfacial oxide, electrons will flow from the CdO into both the oxide layer and n-InP. The realignment of Fermi levels changes the band diagram to panel (c) of Figure 6, where ϕ_B is the contact barrier height. The barrier caused by the interfacial oxide layer explains the Schottky behavior of the contact. The resistance across the contact is proportional to ϕ_B, which in turn is proportional to $\phi_{sub} - \phi_{CdO}$. The contact resistance for CdO:Sn should be higher than of CdO because $\phi_{CdO:Sn} < \phi_{CdO}$. When pretreated with O_2 plasma, the thickness of the oxide layer on the InP increases (Figure 6c), which will result in an increase in ϕ_{sub} and subsequently increase ϕ_B. Hence, the samples pretreated with O_2 plasma are more resistive.

If the Schottky behavior is caused by the interfacial oxide layer, the removal or sufficient reduction of the oxide should permit ohmic contact (Figure 6c); when the barrier thickness W is thin enough, electrons can tunnel through the barrier giving ohmic contact. Frequently, oxide-layers can be reduced by an H_2 plasma.[56−58] Both CdO and CdO:Sn films were deposited on H_2 plasma cleaned InP and contacts formed. The current−voltage curves for contacts with a 60 μm gap distance are shown in panel (c) of Figure 5; it is easily seen that samples with H_2 plasma pretreatment achieve ohmic contact. The higher resistance (flatter $I-V$ curve) of the CdO:Sn contacts is due to the larger free-band offset between $\phi_{CdO:Sn}$ and ϕ_{InP} rather than that for ϕ_{CdO} and ϕ_{InP}.[32]

The dynamic resistance, as calculated from $I-V$ curves such as those in panel (c) of Figure 5, is the total resistance (R_{tot}); in addition to the InP/CdO contact resistances, it includes the resistances due to the probes, metal pads, CdO film, InP substrate, and probe/metal and metal/CdO interfaces. The dynamic resistance due to the two probes and two probe/gold interfaces is measured to be ~1.98 Ω. The effect of the InP substrate could be removed by simulation. The simulation of the InP substrate resistance and the calculation of the contact resistance are explained in details in the Supporting Information. Correcting for the probe and InP substrate effects, the InP/CdO and InP/CdO:Sn contact resistances are calculated.to be $(1.7 \pm 0.7) \times 10^{-2}$ Ω and $(9.0 \pm 1.5) \times 10^{-2}$ Ω for CdO and CdO:Sn, respectively. Taking the contact area into consideration, the corresponding contact resistance is $(6.8 \pm 2.8) \times 10^{-6}$ Ω cm^2 and $(3.6 \pm 0.6) \times 10^{-5}$ Ω cm^2.

CONCLUSION

We have achieved good ohmic contact with low contact resistance to an n-InP substrate with a TCO using intrinsically doped CdO and Sn-doped CdO thin films. Different surface pretreatments of the n-InP prior to the PLD growth of the CdO (CdO:Sn) were investigated. The pretreatment of the substrate surface with an O_2 plasma prior to CdO (CdO:Sn) deposition increases the Schottky nature of the junction. The pretreatment of the substrate surface with an H_2 plasma prior to CdO (CdO:Sn) deposition is key to obtaining ohmic contact. This is consistent with the thickening of an oxide interfacial layer with O_2 plasma and a thinning of an oxide interfacial layer with H_2 plasma. The measured contact resistance for the H_2 plasma-treated samples is as low as $(6.8 \pm 2.8) \times 10^{-6}$ Ω cm^2 and $(3.6 \pm 0.6) \times 10^{-5}$ Ω cm^2 for CdO and CdO:Sn samples, respectively. The experiment result indicates promise for the use of CdO thin films as a TCO contact material for developing novel high performance optoelectronic, nanophotonic, and electronic devices.

ASSOCIATED CONTENT

Supporting Information. Information on how contact resistance is obtained is explained in detail. This material is available free of charge via the Internet at http://pubs.acs.org.

AUTHOR INFORMATION

Corresponding Author

*E-mail: f-ou@northwestern.edu.

ACKNOWLEDGMENT

This research was supported by the MRSEC program of NSF (DMR-0520513) at the Northwestern University Materials Research Center.

REFERENCES

(1) Loualiches, S.; Lharidon, H.; Lecorre, A.; Lecrosnier, D.; Salvim, M.; Favennec, P. N. *Appl. Phys. Lett.* **1988**, *52*, 540–542.
(2) Gleason, K. R.; Dietrich, H. B.; Henry, R. L.; Cohen, E. D.; Bark, M. L. *Appl. Phys. Lett.* **1978**, *32*, 578–581.
(3) Shorubalko, I.; Xu, H. Q.; Maximov, I.; Nilsson, D.; Omling, R.; Samuelson, L.; Seifert, W. *IEEE Electron Device Lett.* **2002**, *23*, 377–379.
(4) Dvorak, M. W.; Bolognesi, C. R.; Pitts, O. J.; Watkins, S. P. *IEEE Electron Device Lett.* **2001**, *22*, 361–363.
(5) Shibata, J.; Nakao, I.; Sasai, Y.; Kimura, S.; Hase, N.; Serizawa, H. *Appl. Phys. Lett.* **1984**, *45*, 191–193.
(6) Hafez, W.; Feng, M. *Appl. Phys. Lett.* **2005**, *86*, 152101.
(7) Endoh, A.; Yamashita, Y.; Shinohara, K.; Hikosaka, K.; Matsui, T.; Hiyamizu, S.; Mimura, T. *Jpn. J. Appl. Phys.* **2003**, *42*, 2214–2218.
(8) Ho, P.; Kao, M. Y.; Chao, P. C.; Duh, K. H. G.; Ballingall, J. M.; Alllen, S. T.; Tessmer, A. I.; Smith, P. M. *Electron. Lett.* **1991**, *27*, 325–327.
(9) Dawson, D.; Samoska, L.; Fung, A. K.; Lee, K.; Lai, R.; Grundbacher, R.; Liu, P. H.; Raja, R. *IEEE Microwave Wireless Compon. Lett.* **2005**, *15*, 874–876.
(10) Yamaguchi, M. *J. Appl. Phys.* **1995**, *78*, 1476–1480.
(11) Rech, B.; Wagner, H. *Appl. Phys. A: Mater. Sci. Process.* **1999**, *69*, 155–167.
(12) van de Lagemaat, J.; Park, N. G.; Frank, A. J. *J. Phys. Chem. B* **2000**, *104*, 2044–2052.
(13) Coldren, L. A. *IEEE J. Sel. Top. Quant. Electron.* **2000**, *6*, 988–999.
(14) Liu, Y. J.; Yen, C. H.; Hsu, C. H.; Yu, K. H.; Chen, L. Y.; Tsai, T. H.; Liu, W. C. *Opt. Rev.* **2009**, *16*, 575–577.
(15) Bashar, S. A.; Rezazadeh, A. A. *IEEE Trans. Microwave Theory Tech.* **1995**, *43*, 2299–2303.
(16) Chopra, K. L.; Major, S.; Pandya, D. K. *Thin Solid Films* **1983**, *102*, 1–46.
(17) Freeman, A. J.; Poeppelmeier, K. R.; Mason, T. O.; Chang, R. P. H.; Marks, T. J. *MRS Bull.* **2000**, *25*, 45–51.
(18) Hartnagel, H. L.; Dawar, A. L.; Jain, A. K.; Jagadish, C. *Semiconducting Transparent Thin Films*; Institute of Physics Publishing: Bristol, U.K., 1995.
(19) Gordon, R. G. *MRS Bull.* **2000**, *25* (8), 52–57.
(20) Ueda, N.; Maeda, H.; Hosono, H.; Kawazoe, H. *J. Appl. Phys.* **1998**, *84*, 6174–6177.
(21) Yang, Y.; Jin, S.; Medvedeva, J. E.; Ireland, J. R.; Metz, A. W.; Ni, J.; Hersam, M. C.; Freeman, A. J.; Marks, T. J. *J. Am. Chem. Soc.* **2005**, *127*, 8797–8804.
(22) Yi, F.; Ou, F.; Liu, B.; Huang, Y.; Ho, S. T.; Wang, Y.; Liu, J.; Marks, T. J.; Huang, S.; Luo, J.; Jen, A. K. Y.; Dinu, R.; Jin, D. *Opt. Express* **2010**, *18*, 6779–6796.
(23) Nunoya, N.; Nakamura, M.; Morshed, M.; Tamura, S.; Arai, S. *IEEE J. Sel. Top. Quant. Electron.* **2001**, *7*, 249–258.
(24) Irmscher, S.; Lewen, R.; Eriksson, U. *IEEE Photon. Technol. Lett.* **2002**, *14*, 923–925.
(25) Masona, T. O.; Gonzaleza, G. B.; Kammlerb, D. R.; Mansourian-Hadavia, N.; Ingram, B. J. *Thin Solid Films* **2002**, *411*, 106–114.
(26) Yan, M.; Lane, M.; Kannewurf, C. R.; Chang, R. P. H. *Appl. Phys. Lett.* **2001**, *78*, 2342–2344.
(27) Chen, K. J.; Enoki, T.; Maezawa, K.; Arai, K.; Yamamoto, M. *IEEE Trans. Electron Devices* **1996**, *43*, 252–257.
(28) Del Alamo, J. A.; Mizutani, J. *Solid-State Electron.* **1988**, *31*, 1635–1639.
(29) Minami, T *Semicond. Sci. Technol.* **2005**, *20*, 35–44.
(30) Lin, H. C.; Senanayake, S.; Cheng, K. Y.; Hong, M.; Kwo, J. R.; Yang, B.; Mannaerts, J. P. *IEEE Trans. Electron Devices* **2003**, *50*, 880–885.
(31) Blank, T. V.; Gol'dberg, Y. A. *Semiconductors* **2007**, *41*, 1281–1308.
(32) Wang, S. *Fundamentals of Semiconductor Theory and Device Physics*; Prentice Hall, Upper Saddle River, NJ, 1989.
(33) Physical Properties of Semiconductors, Ioffe Physico-Technical Institute. http://www.ioffe.ru/SVA/NSM/Semicond/index.html.
(34) Xu, Y.; Schoonen, M. A. A. *Am. Mineral.* **2000**, *85*, 543–556.
(35) Dou, Y.; Egdell, R. G.; Walker, T.; Law, D. S. L.; Beamson, G. *Surf. Sci.* **1998**, *398*, 241–258.
(36) Dou, Y.; Fishlock, T.; Egdell, R. G.; Law, D. S. L.; Beamson, G. *Phys. Rev. B* **1997**, *55*, R13381–R13384.
(37) Moss, T. S. *Proc. Phys. Soc., London, Sect. B* **1954**, *67*, 775–782.
(38) Burstein, E. *Phys. Rev.* **1954**, *93*, 632–633.
(39) Hamberg, I.; Granqvist, C. G.; Berggren, K. F.; Sernelius, B. E.; Engström, L. *Phys. Rev. B* **1984**, *30*, 3240–3249.
(40) Jefferson, P. H.; Hatfield, S. A.; Veal, T. D.; King, P. D. C.; McConville, C. F.; Zúñiga Pérez, J.; Muñoz Sanjosé, V. *Appl. Phys. Lett.* **2008**, *92*, 022101.
(41) Makuta, I. D.; Poznyak, S. K.; Kulak, A. I. *J. Phys. Chem. Solids* **1994**, *55*, 447–451.
(42) Benko, F. A.; Koffyberg, F. P. *Solid State Commun.* **1986**, *57*, 901–903.
(43) Gurumurugan, K.; Mangalaraj, D.; Narayandass, S. K.; Nakanishi, Y. *Mater. Lett.* **1996**, *28*, 307–312.
(44) Li, X.; Young, D. L.; Moutinho, H.; Yan, Y.; Narayanswamy, C.; Gessert, T. A.; Couttsz, T. J. *Electrochem. Solid-State Lett.* **2001**, *4*, C43–C46.
(45) Buchholz, D. B.; Liu, J.; Marks, T. J.; Zhang, M.; Chang, R. P. H. *ACS Appl. Mater. Interfaces* **2009**, *1*, 2147–2153.
(46) Subramanyam, T. K.; Uthanna, S.; Naidu, B. S. *Mater. Lett.* **1998**, *35*, 214–220.
(47) Vigil-Galán, O.; Sánchez-González, Y.; Arias-Carbajal, A.; Contreras-Puente, G.; Tufiño-Velázquez, M.; Ruiz, C. M. *Phys. Status Solidi A* **2006**, *203*, 3713–3719.
(48) Ellmer, K. *J. Phys. D: Appl. Phys.* **2001**, *34*, 3097–3108.
(49) Kulkarni, A. K.; Schulz, K. H.; Lim, T. S.; Khan, M. *Thin Solid Films* **1999**, *345*, 273–277.
(50) Seto, J. Y. W. *J. Appl. Phys.* **1975**, *46*, 5247–5254.
(51) Brunfaux, J.; Cachet, H.; Froment, M.; Messad, A. *Thin Solid Films* **1991**, *197*, 129–142.
(52) Saha, B.; Thapa, R.; Chattopadhyay, K. K. *Solid State Commun.* **2008**, *145*, 33–37.
(53) Guivarc'h, A.; L'Haridon, H.; Pelous, G.; Hollinger, G.; Pertosa, P. *J. Appl. Phys.* **1984**, *55*, 1139–1148.
(54) Hattori, K.; Izumi, Y. *J. Appl. Phys.* **1981**, *52*, 5699–5701.
(55) Gagnaire, A.; Joseph, J.; Etcheberry, A.; Gautron *J. Solid-State Sci. Technol.* **1985**, *132*, 1655–1658.
(56) Tu, C. W.; Chang, R. P. H.; Schlier, A. R. *Appl. Phys. Lett.* **1982**, *41*, 80–81.
(57) Hofstra, P. G.; Robinson, B. J.; Thompson, D. A.; McMaster, S. A. *J. Vac. Sci. Technol., A* **1995**, *13*, 2146–2150.
(58) Bruno, G.; Capezzuto, P.; Losurdo, M. *Phys. Rev. B* **1996**, *54*, 17175–17183.